Faraday Discussions

Accepted Manuscript

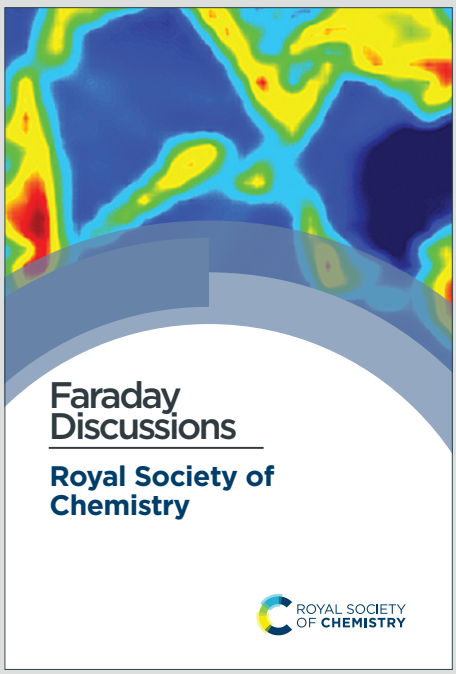

This article can be cited before page numbers have been issued, to do this please use: D. G. Stavenga, M. Staal and C. J. van der Kooi, *Faraday Discuss.*, 2020, DOI: 10.1039/D0FD00055H.

ROYAL SOCIETY OF CHEMISTRY

www.rsc.org/faraday_d

Conical epidermal cells cause velvety colouration and enhanced patterning in *Mandevilla* flowers

View Article Online
DOI: 10.1039/D0FD00055H

Doekele G. Stavenga[1], Marten Staal[2], Casper J. van der Kooi[2]

[1] Surfaces and thin films, Zernike Institute for Advanced Materials, University of Groningen, NL-9747 AG Groningen, the Netherlands

[2] Groningen Institute for Evolutionary Life Sciences, University of Groningen, NL-9747 AG Groningen, The Netherlands

ORCIDs: 0000-0002-2518-6177 (DGS); 0000-0003-0613-7633 (CJvdK)

Contact: D.G.Stavenga@rug.nl, C.J.van.der.Kooi@rug.nl

Summary

The majority of angiosperms have flowers with conical epidermal cells, which are assumed to have various functions, such as enhancing the visual signal to pollinators, but detailed optical studies on how conical epidermal cells determine the flower's visual appearance are scarce. Here we report that conical epidermal cells of *Mandevilla sanderi* flowers effectively reduce surface gloss and create a velvety appearance. Owing to the reduction in surface gloss, the flower further makes more efficient use of floral pigments and light scattering structures inside the flower. The interior backscattering yields a cosine angular dependence of reflected light, meaning the flowers approximate near-perfect (Lambertian) diffusers, creating a visual signal that is visible across a wide angular space. Together with the large flowers and the tilted corolla tips this generates a distinct visual pattern, which may enhance the visibility to pollinators.

Keywords: Lambertian diffuser, pollination, angle-dependent spectrophotometry, vision, *Dipladenia*

Introduction

The vast majority of angiosperms have flowers with conical epidermal cells, which may have different roles in pollination. For example, conical epidermal cells may reduce petal wettability and/or provide grip or tactile cues to landing insect pollinators [1, 2]. Another hypothesis for the function of the cones is that they act as small lenses, so to enhance light capture by the pigments in the epidermal cells and increase colour contrast [3-6]. However, conical epidermal cells

DOI: 10.1039/D0FD00055H

generally vary in size and spacing and how that, particularly under natural conditions where the illumination varies, determines possible optical effects is unknown [7].

Here, we forward a new function of conical epidermal cells, namely that cones reduce surface gloss and so increase the flower's contrast. We have chosen *Mandevilla sanderi* (also known as *Dipladenia*) flowers to study the optical characteristics of conically-shaped epidermal cells, because the flowers, when observed from various directions, display distinctly varying reflection patterns with a velvety appearance. This intriguing phenomenon presumably has a structural origin, which inspired us to further investigate the flowers' spatial colouration characteristics.

Mandevilla plants, also known as rocktrumpets, are popular garden plants due to their strikingly coloured, large flowers. The genus *Mandevilla* belongs to the family Apocynaceae, and its members differ in floral traits such as corolla shape, colour and size [8]. *Mandevilla* species are pollinated by different guilds of pollinators, including bees [9], hummingbirds [10] and hawkmoths [11, 12]. Notably the Sundaville varieties of *Mandevilla sanderi* have large flowers with a five-lobed corolla, brightly red, pink, yellow or white coloured. The 'Sundaville Red' variety has a deep-red colour due to strongly anthocyanin-pigmented epidermal cells. The cone shape of the flower's epidermal cells is similar in size and shape as those found in flowers of many species [4, 13-15]. Measurements of the flowers' reflectance spectra show that the conical shape of the adaxial epidermal cells effectively reduces gloss, especially when observed under large angles. As a consequence, tilted corolla tips become much darker than untilted lobe areas, and in this way contrastful, velvety flower patterns are created.

Materials and Methods

Plant material, photography, and anatomy

Two 'Sundaville Red' *Mandevilla sanderi* plants were obtained from a commercial supplier., The anatomical, reflection and pigmentation characteristics of the plants were very similar. Macro-photographs of the flowers were made with a Canon DC7 digital camera. To visualize the location of the red pigment, flower pieces were embedded in a 6% agarose solution at a temperature of approximately 55 °C, i.e. close to the temperature of agarose solidification. Micrographs of transverse sections were made subsequently with a Zeiss Universal microscope (Zeiss, Oberkochen, Germany), equipped with an Epiplan 16/0.35 objective and a DCM50 camera (Mueller-Optronic, Erfurt, Germany). The microscope was also used for photographing the reflection and transmission of flower lobes.

Spectrophotometry

Reflectance spectra were measured as a function of angle of light incidence and reflection in a goniometric setup with two rotatable optical fibers. One fiber delivered light from a xenon lamp to the object, and the other fiber collected the reflected light and guided it to an AvaSpec-2048 spectrometer (Avantes, Apeldoorn, the Netherlands). The angular resolution of the setup has a Gaussian shape with half-width ~5º [16]. All measured spectra were divided by the spectrum obtained from a white diffuse reflectance standard (WS-2, Avantes), which was illuminated normally while the detector was also positioned in the normal direction. The measurements were mainly performed with unpolarized light on five lobes, yielding very similar results.

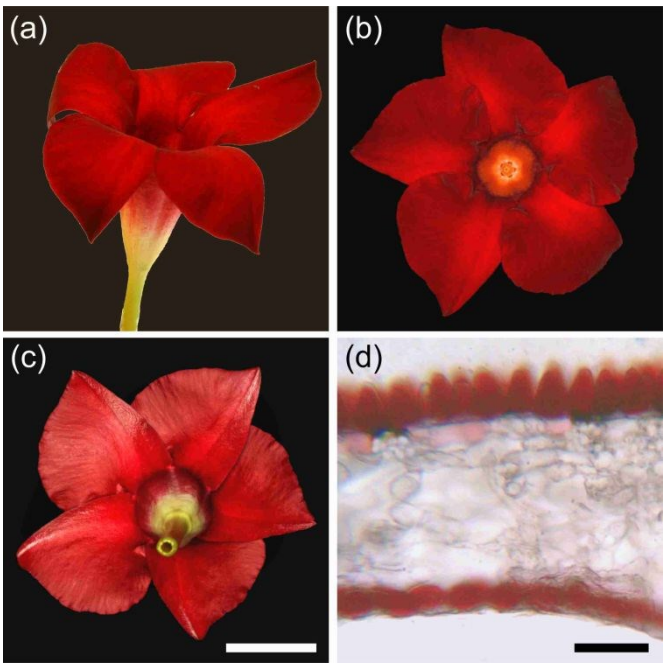

Fig. 1. *Mandevilla* 'Sundaville Red' flower. (a) Lateral view. (b) Upper side view. (c) Underside view. (d) Lobe section embedded in agarose. Scale bars: (a-c), 2 cm; (d), 50 µm.

Results

Flower structure and the shape of epidermal cells

The Red morph of the *Mandevilla* flower has a five-lobed corolla, coloured deep-red (Fig. 1). While the adaxial side of the lobes is matt (Fig. 1a,b), with varying brightness across the lobes' plane, the abaxial side is glossy (Fig. 1c). Cross-sections of the Red morph's lobes revealed that the colour is due to pigment concentrated in both the adaxial (upper) and abaxial (lower) epidermis (Fig. 1d). The adaxial epidermal cells have a distinctly conical-papillate shape, but the abaxial epidermal cells are only slightly convex. The mesophyll in between the epidermises is interspersed with large air holes (Fig. 1d).

View Article Online
DOI: 10.1039/D0FD00055H

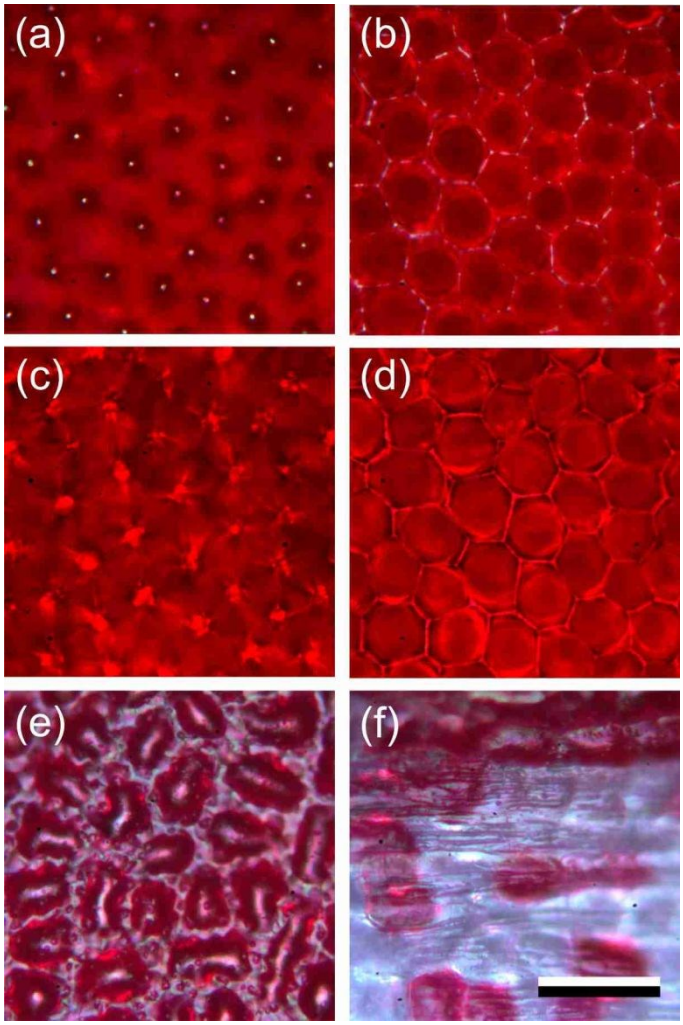

Fig. 2. Close-up views of the lobe epidermis of the Red morph. (a) Focus at the adaxial cone tips. (b) Level of cone cell borders. (c) Level of focal points of the cone cells. (d) Level of cone cell borders. (e) Heavily pigmented area of lower epidermis. (f) Sparsely pigmented area proximally in the lower epidermis in the transition zone of lobe and tube. (a-d) adaxis; (e, f) abaxis; (a, b, e, f) epi-illumination; (c, d) transmitted light. Scale bar: (a-f), 50 µm.

Due to the different shapes of the epidermal cells, the adaxial and abaxial surfaces have a different appearance. When observed with an epi-illumination light microscope, the conical cells of the adaxial epidermis appear to be rather orderly arranged in an about hexagonal lattice. Focusing at the level of the cone tips reveals distinct surface reflections (Fig. 2a), and at a deeper level the conical cell borders emerge (Fig. 2b). When changing the epi-illumination to transmitted light, bright dots occur at a level about halfway in between the cell tips and borders, clearly marking the level of the focal points of the conical cells (Fig. 2c). Focusing at the level of the cell borders, the transmitted light shows bright border lines surrounding dark-red circles (Fig. 2d), indicating that the red pigment is homogeneously distributed in the cone cells, in agreement with the anatomy of Fig. 1d.

Epi-illumination of the abaxial side shows the more or less random arrangement of the red-pigmented epidermal cells (Fig. 2e). The picture is glossy, due to the fairly smooth surface of the slightly convex epidermal cells (Fig. 1d). In the more proximal corolla area, in the transition zone of the lobe to the tube, the pigmentation of the abaxial epidermal cells vanishes stochastically (Fig. 2f), so that a greenish to colourless tube and peduncle remain (Fig. 1a,c).

Reflectance spectra of the different flower areas

To better understand the optical mechanisms causing the different appearances of the matt adaxial and glossy abaxial lobe sides, we studied the spectral characteristics of the corolla lobes using angle dependent reflectance measurements. We applied spectrophotometry to both the adaxial and abaxial side of the corolla lobes using a goniometric setup with two rotatable fibers, one delivering the illumination and the other collecting the reflected light, while systematically varying the illumination or detection angle.

We firstly applied normal illumination and measured the reflectance at various reflection angles (Fig. 3a; see inset). For all angles of reflection, the reflectance of the lobe's adaxial side is very low throughout the main visible wavelength range. In the longer wavelength range, the reflectance is high, but it decreases monotonically with an increasing angle of reflection (Fig. 3a). The reflectance of the abaxial side, when measured with the same procedure, is much higher, especially for normally incident light (Fig. 3b). To assess the angle dependence of the reflectance of both flower sides, we evaluated the reflectance at 550 and 750 nm separately (Fig. 3c,d). Clearly, the adaxial reflectance at 550 nm (R_{550}) is negligible for all reflection angles (Fig. 3a,c), but the abaxial R_{550} is considerable for angles up to ~30º (Fig. 3d, blue curve); the latter is due to the surface gloss (Fig. 3b,d). Given the floral pigment absorbs strongly between 300 and 600 nm, the R_{550} is fully due to surface reflections. Assuming that this surface gloss is the same for all wavelengths, subtracting R_{550} from the reflectance at 750 nm (R_{750}) yields the backscattering from the lobe interior, $R_i = R_{750} - R_{550}$, which well approximates a cosine function for both the adaxial and abaxial side (Fig. 3c,d). Such a cosine-angular dependence of the reflectance is characteristic of a Lambertian, matte and diffusely reflecting surface, indicating that the flower interior approximates an ideal reflecting diffuser. Yet, for a perfect Lambertian diffuser, the amplitude at normal illumination is 1 whereas for the lobe interior it is 0.42, which is due to the limited thickness of the lobe.

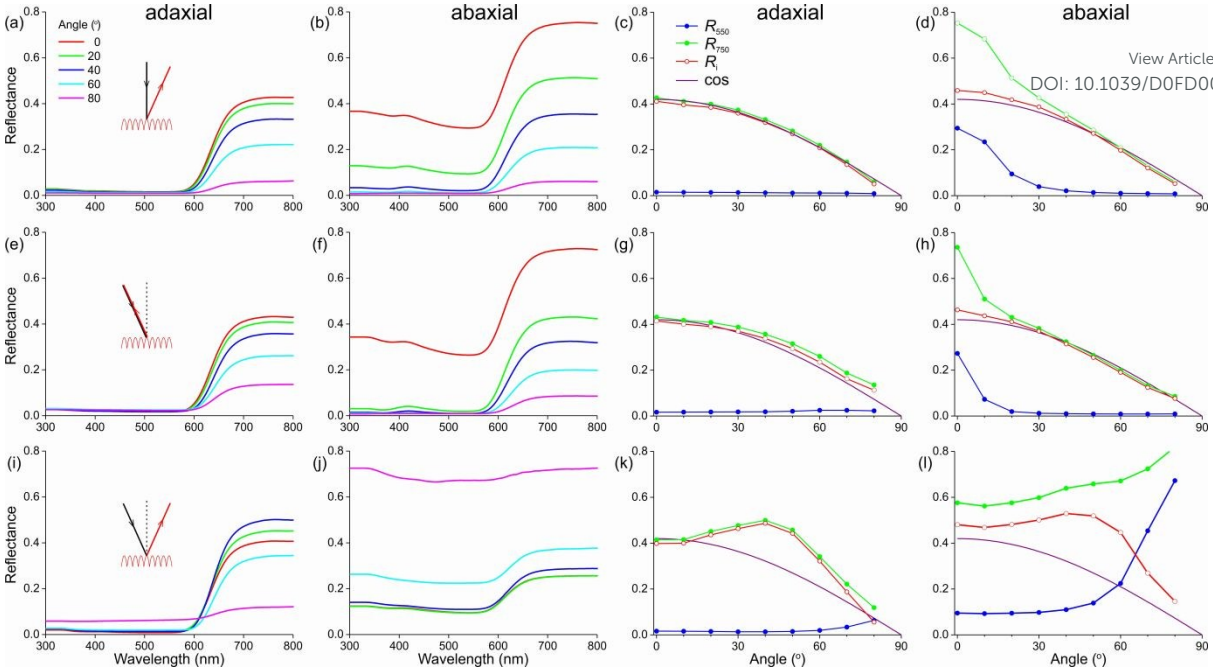

Fig. 3. Angle-dependent reflectance of the adaxial and abaxial side of a Red morph corolla lobe. (a-d) Illumination (inset, black) normal and stable; detector angle (inset, red) varying. (e-h) Illumination and detector angle identical and varying. (i-l) Illumination and detector under different angles symmetrical with respect to the normal. (a, b, e, f, i, j) Reflectance spectra measured at angles 0º, 20º, 40º, 60º, and 80º with respect to the normal. (c, d, g, h, k, l) Reflectance values at 550 and 750 nm (R_{550} and R_{750}) and their difference ($R_i = R_{750} - R_{550}$) as a function of the detector angle, compared with a cosine function (cos). (a, c, e, g, i, k) Measurements at adaxial side. (b, d, f, h, j, l) Measurements at abaxial side.

We subsequently varied the illumination angle and measured the light reflected into the same angle (Fig. 3e; see inset). The reflectance spectra measured for the adaxial and abaxial side were surprisingly similar to those of the previous case where the illumination was always normal. Indeed, processing the spectral data in the same way as above revealed that the reflectance difference $R_i = R_{750} - R_{550}$ approximated the same cosine function as that of Fig. 3c,d (Fig. 3g,h). Only the angular spread of R_{550} was now slightly narrower (compare Fig. 3h with 3d).

In a third approach, we positioned the illumination and detector into opposite, mirror angles (Fig. 3i-l). The reflectance of the adaxial side measured this way was in the main part of the visible wavelength range again minimal except for extremely oblique angles, in other words, R_{550} was minor except for angles > 70º (Fig. 3k). However, the angle-dependence of the reflectance component due to backscattering by the flower's interior, R_i, deviated from the cosine function, showing a slightly enhanced reflectance for angles of incidence and reflection around 40º (Fig. 3k).

The abaxial reflectance behaved very differently. The considerable reflectance throughout the whole wavelength range rapidly increased with increasing angle of light incidence and reflection (Fig. 3j). When subtracting the measured abaxial R_{550} from R_{750}, the resulting angle dependence of the interior reflectance was highly similar to the corresponding data deduced for the adaxial side (red curves in Fig. 3k and Fig. 3i), meaning that the arrangement of interior structures is about random. However, for low values of the angle of incidence R_{550} was about constant, but it rapidly rose for angles > 45º, yielding reflectance values > 1 for angles > 60º. These unrealistically high values were obtained because the spectrum of a normally-illuminated, ideal-diffuser was used as the reference. The assumed criterion of a diffuser holds for the adaxial surface (Fig. 3c), but for the abaxial surface it holds also only when the angles of light incidence and reflection widely differ, i.e. > 30º (e.g. Fig. 3d,h). Therefore, when measuring the reflectance of the abaxial flower surface in the mirror angle, the detector will capture a large fraction of the surface reflections in addition to the (comparatively low) backscattering of the lobe interior. We estimated that the specularity of the abaxial side causes an overestimate of the reflectance with a factor ~3, and we therefore present in Fig. 3j the measured spectra divided by 3. Figure 3f contains the associated values of R_{550} (as well as the values of R_{750}, now being the sum of R_i and R_{550}).

To ascertain that the reflectances of the abaxial side measured in the short-wavelength range were indeed virtually fully due to the surface reflections, as a control we also performed the same series of measurements using polarized light, by fitting the detector fiber with a linear analyzer. The R_{550} data for TE- and TM-polarized light (that is, polarized perpendicular and parallel to the plane of light incidence, respectively) were as expected for a reflecting dielectric medium, with the TE-reflectance rising monotonically and the TM-reflectance going to zero for an angle of light incidence ~60º. As expected for a diffuser, the interior reflectance R_i was virtually independent of the polarization (not shown).

Discussion

Our analysis of the angle-dependent reflections of the *Mandevilla* flowers demonstrates that two clearly distinguishable mechanisms contribute to the flower reflectance, i.e. firstly the reflecting surface and secondly the flower interior that backscatters incident light. The conclusion that both the surface and interior of flowers contribute to the visual signal has been shown before [4, 7, 17-19], but the relative contributions of the surface and interior and how they depend on the angles of illumination and observation has remained virtually unstudied.

We found for the adaxial flower side that the surface reflections are minimal in the wavelength range up to ~600 nm for all angles of light incidence and reflection. Therefore, the considerable reflectance measured in the long-wavelength range must be due to scattering inhomogeneities in the flower interior. The interior backscattering results in a cosine angular dependence of the diffused light, i.e. highly similar to the case of a Lambertian surface. For the abaxial side, the about smooth surface creates reflections that are far from negligible, and even creates a slightly metallic lustre, which can be found in other species also [20, 21]. When illuminated with a narrow-aperture light source, the abaxial surface reflections show a minor angular spread (halfwidth 10-15º), owing to the slightly convex surfaces of the abaxial epidermal cells.

Whereas the reflections of the adaxial and abaxial flower surfaces are very different, the light backscattered by the interior as seen from the adaxial and abaxial sides are remarkably similar (Fig. 3d,h,l). Furthermore, for both sides, when the angle of light incidence and reflection are equal but opposite, the angular dependence of the interior reflectance modestly departs from that of an ideal diffuser. Presumably the directional component of the reflectance is due to some planar arrangement of the lobe's interior structures, such as the stratification of interior cell layers.

The cosine angle dependence of the long-wavelength reflectance has interesting consequences for flowers with tilted tips, as is the case for the *Mandevilla* flowers (Fig. 1). The corolla features a contrasting pattern, in spite of the uniform red pigmentation across the corolla lobes. In principle this could also be the case when observing the abaxial side of the flower lobe, but the gloss of the surface reflections drowns the interior reflections. Furthermore, as the gloss is about wavelength independent, it will severely diminish the colour contrast, which is a critical aspect for detection by insect pollinators [7].

The epidermal cone cells thus have a crucial function in reducing gloss and enhancing colour contrast via two different optical processes. A long-standing hypothesis is that enhanced colouration is achieved by light focusing onto the pigment [3, 4, 22]. The ridges of the elongated petal epidermal cells of the California poppy (*Eschscholzia californica*) have been attributed a similar colour-enhancing function [22]. We may note that the cones indeed can function as lenses (Fig. 2c), but the focusing will strongly depend on the direction of the incident light, so that with wide-angled, natural illuminations there is no distinct focusing. Thus rather than having a focusing function, the actual optical function of the cone-shaped adaxial epidermal cells is to effectively annihilate the gloss, which undermines the colour contrast that is pivotal in visual detection of flowers by pollinators [7].

In addition to reducing surface gloss, a decreased surface reflectance means more light will enter the flower and reach the floral pigments. This will have severe effects especially for incident light at oblique angles. A larger fraction of incident light entering the flower interior results in an increased backscattering by the diffusing structural components. Further, light that enters the flower will be filtered by pigments present in the epidermal cell layer (Figure 1d). When the light is subsequently backscattered by the interior structures it traverses the pigment layer a second time[18], meaning that the light reflected by the flower interior will be modulated even more and exhibit a high colour contrast against the surrounding vegetation. In summary, instead of having a focusing function, conical epidermal cells enhance colour contrast by both decreasing surface gloss and increasing long-wavelength reflectance.

A contrasting case is that of buttercups, which instead of decreasing surface reflectance increase the adaxial epidermal reflection. Their adaxial epidermis is a carotenoid-filled, thin film in air, which causes a high, yellow reflectance [23, 24]. The petals of buttercups form together a paraboloid mirror, and as the flowers are heliotropic, they keep sun light focused at the reproductive organs, presumably to increase flower temperature [24]. This mechanism will not work in flowers with a spread-out corolla for which a rough surface is then advantageous.

Gloss reduction by roughening the surface is a widespread trait also in the animal kingdom, for reducing the specularity and/or enhancing transmittance [25-28]. Additional or alternative roles for rough flower surfaces can be, for example, anti-wettability and self-cleaning [15, 29, 30]. Furthermore, the conical epidermal cells of flowers may enhance grip to landing insect pollinators [2, 19], but this is not underscored by the recent finding that flowers pollinated by landing insects (bees and flies) do not have more cone-shaped surfaces than flowers pollinated by animals that do not land on flower surfaces (birds and hawkmoths) or via self-pollination [14].

A main function of the conically-shaped adaxial cells of the adaxial epidermis will be to create a visual signal that is widely visible and in case of large, pleated and deeply-pigmented flowers to create contrastful patterning in the lobe. The increase of within-flower colour contrast and the scattering of light into a wide angular space will increase the flower's visibility to pollinators. How conical cells contribute to colour formation in species with other pigmentation and how that enhances flower salience in natural conditions provides an intriguing avenue for future research.

Acknowledgements We thank Dr Bodo Wilts for providing constructive comments and Hein Leertouwer for technical assistance. This study was financially supported by the

AFOSR/EOARD (grant FA9550-15-1-0068, to DGS) and NWO (Veni grant 016.Veni.181.025, to CJvdK).

References

1 P. G. Kevan and M. A. Lane, *Proc. Natl. Acad. Sci. U. S. A.,* 1985, **82**, 4750-4752.

2 H. M. Whitney, K. V. Bennett, M. Dorling, L. Sandbach, D. Prince, L. Chittka and B. J. Glover, *Ann. Bot.,* 2011, **108**, 609-616.

3 F. Exner and S. Exner, *Sitzungsber. Kais. Akad. Wiss. Wien, Math.-Nat. Kl. I,* 1910, **119**, 191-245.

4 Q. Kay, H. Daoud and C. Stirton, *Bot. J. Linn. Soc.,* 1981, **83**, 57-83.

5 R. A. Bone, D. W. Lee and J. Norman, *Appl. Opt.,* 1985, **24**, 1408-1412.

6 T. C. Vogelmann, J. F. Bornman and D. J. Yates, *Physiol. Plantarum,* 1996, **98**, 43-56.

7 C. J. van der Kooi, A. G. Dyer, P. G. Kevan and K. Lunau, *Ann. Bot.,* 2019, **123**, 263-276.

8 L. De Araújo, Z. Quirino and I. Machado, *Plant Biol.,* 2014, **16**, 947-955.

9 C. Löhne, I. C. Machado, S. Porembski, C. Erbar and P. Leins, *Bot. Jahrb*., 2004, **125**, 229-243.

10 F. G. Stiles and C. E. Freeman, *Biotropica,* 1993, **25**, 191-205.

11 M. Moré, A. N. Sérsic and A. A. Cocucci, *Ann. Mo. Bot. Gard.,* 2007, **94**, 485-505.

12 A. Rubini Pisano, M. Moré, M. A. Cisternas, R. A. Raguso and S. Benitez-Vieyra, *Plant Biol.,* 2019, **21**, 206-215.

13 P. Bräuer, C. Neinhuis and D. Voigt, *Arthropod Plant Interact.,* 2017, **11**, 171-192.

14 M. Kraaij and C. J. van der Kooi, *Plant Biol.,* 2020, **22**, 177-183.

15 A. Watanabe-Taneda and H. Taneda, *Flora,* 2019, **257**, 151417.

16 D. G. Stavenga, B. D. Wilts, H. L. Leertouwer and T. Hariyama, *Phil. Trans. R. Soc. B,* 2011, **366**, 709-723.

17 S. Vignolini, M. P. Davey, R. M. Bateman, P. J. Rudall, E. Moyroud, J. Tratt, S. Malmgren, U. Steiner and B. J. Glover, *New Phytol.,* 2012, **196**, 1038-1047.

18 D. G. Stavenga and C. J. van der Kooi, *Planta,* 2016, **243**, 171-181.

19 S. Papiorek, R. R. Junker and K. Lunau, *PloS One,* 2014, **9**, e112013.

20 Y. Zhang, T. Hayashi, M. Hosokawa, S. Yazawa and Y. Li, *Sci. Hort.,* 2009, **121**, 213-217.

21 Y. Zhang, T. Sun, L. Xie, T. Hayashi, S. Kawabata and Y. Li, *J. Plant Res.,* 2015, **128**, 623-632.

22 B. D. Wilts, P. J. Rudall, E. Moyroud, T. Gregory, Y. Ogawa, S. Vignolini, U. Steiner and B. J. Glover, *New Phytol.,* 2018, **219**, 1124-1133.

23 S. Vignolini, M. M. Thomas, M. Kolle, T. Wenzel, A. Rowland, P. J. Rudall, J. J. Baumberg, B. J. Glover and U. Steiner, *J. Roy. Soc. Interface,* 2012, **9**, 1295-1301.

24 C.J. van der Kooi, J. T. M. Elzenga, J. Dijksterhuis and D. G. Stavenga, *J. Roy. Soc. Interface* 2017, **14**, 20160933.

25 I. R. Hooper, P. Vukusic and R. Wootton, *Opt. Express,* 2006, **14**, 4891-4897.

26 M. Spinner, A. Kovalev, S. N. Gorb and G. Westhoff, *Sci. Rep.,* 2013, **3**, 1846.

27 D. L. Maurer, T. Kohl and M. J. Gebhardt, *Arthropod Struct. Dev.,* 2017, **46**, 147-155.

28 J. Riedel, M. J. Vucko, S. P. Blomberg, S. K. Robson and L. Schwarzkopf, *J. Anat.,* 2019, **234**, 853-874.

29 H. Taneda, A. Watanabe-Taneda, R. Chhetry and H. Ikeda, *Ann. Bot.,* 2015, **115**, 923-937.

30 W. Barthlott and C. Neinhuis, *Planta,* 1997, **202**, 1-8.